研究成果の刊行に関する一覧表

書籍

著者名	題名	編集者名	書籍名	出版社名	出版地	出版年	ページ
Takashi Okamoto	Oxidative Stress in Rheumatoid Arthritis	Young-Joon Surh and Lester Packer0	Oxidative Stress, Inflammation and Health	Marcel Dekker	N.Y USA	2006	In press

雑誌

発表者氏名	論文タイトル	発表誌名	巻号	ページ	出版年
Tozawa,K., Okamoto,T., Kawai,N.,Hashimoto,Y., Nagata,D.,Hayashi,Y., and Kohri,K.	Positive correlation between sialyl Lewis X expression and pathological findings in renal cell carcinoma.	Kidney Int.	67	1391-1396	2005
Sanda, T., Iida, S., Ogura, H., Asamitsu, K., Murata, T., Bacon, K.B. Ueda R., and Okamoto, T.	Growth inhibition of multiple myeloma cells by a novel IkB kinase inhibitor.	Clin. Can. Res.	11	1974-1982	2005
Kobayashi, S., Kajino S., Takahashi,N., Kanazawa, S., Imai, K., Hibi, Y., Ohara, H., Itoh M. and Okamoto,T.	53BP2 induces apoptosis through the mitochondrial death pathway.	Genes Cells	10	253-260	2005
Ota, S., Kanazawa, S., Kobayashi M., Otsuka T. and Okamoto,T.	Establishment of a simple and quantitative immunospot assay for detecting anti-type II collagen antibody using infrared fluorescence imaging system (IFIS).	J. Immunol. Methods	299	189-198	2005
Takahashi, N., Kobayashi, S., Kajino, S., Imai, K., Tomodo, K., Shimizu, S., and Okamoto, T.	Inhibition of the 53BP2S-mediated apoptosis by nuclear factor□B and Bcl-2 family proteins.	Genes Cells.	10	803-811	2005
Imai, K., Nakata, K., Kawai, K., Hamano, T., Mei, N ., Kasai, H. ,and Okamoto, T.	Induction of OGG 1 gene expression by HIV-1 Tat.	J. Biol.Chem.	280	26701-26713	2005
Tanaka, K., Hasegawa, J., Asamitsu, K. and Okamoto, T.	Prevention of the ultraviolet B-mediated skin photoaging by a nuclear factor kB inhibitor parthenolide.	J. Pharmacol. Exp. Ther.	315	624-630	2005

Okamoto,T.	The epigenetic alteration of synovial cell gene expression in rheumatoid arthritis and the roles of NF-kB and Notch signaling pathways.	Mod Rheumatol	15	79-86	2005
Okamoto, T., Sanda, T., and Asamitsu, K.	NF-kB signaling and carcinogenesis.	Curr. Pharm. Design			In press (2006)
Katagiri, D., Hayashi, H., Victoriano, A.F.B., Okamoto, T., and Onozaki, K.	Estrogen stimulates transcription of human immunodeficiency virus type 1 (HIV-1)	Int. Immuno-pharm	6	170-181	2006
Sanda, T., Asamitsu, K., Ogura, H., Iida, S., Utsunomiya, A., Ueda., R., and Okamoto,T.	Induction of cell death in adult T-cell leukemia cells by a novel I κ B kinase inhibitor.	Leukemia			In Press (2006)
Victoriano, A.F.B., Asamitsu,K., Hibi, Y. ,Imai,K. , Barzaga, N.G., and Okamoto, T.	Inhibition of HIV-1 replication in latently infected cells by a novel IkB kinase inhibitor	Antimicrob. Agents Chemother.	50	547-555	2006

別紙５

研究成果の刊行に関する一覧表

書籍

著者氏名	論文タイトル名	書籍全体の編集者名	書籍名	出版社名	出版地	出版年	ページ
なし							

雑誌

発表者氏名	論文タイトル名	発表誌名	巻号	ページ	出版年
Watanabe N, Nishihara Y, Yamaguchi T, Koito A, Miyoshi H, Kakeya H, & Osada H	Fumagillin suppresses HIV-1 infection of macrophage through the inhibition of Vpr activity.	FEBS Letter			2006 (in press)

別紙 5

雑誌

発表者氏名	論文タイトル名	発表誌名	巻号	ページ	出版年
Harashima, N., Tanosaki, R., Shimizu, Y., Kurihara, K., Masuda, T., Okamura, J., and Kannagi, M..	Identification of two new HLA-A*1101-restricted tax epitopes recognized by cytotoxic T lymphocytes in an adult T-cell leukemia patient after hematopoietic stem cell transplantation	J Virol	79	10088-10092.	2005
Kurihara, K., Harashima, N., Hanabuchi, S., Masuda, M., Utsunomiya, A., Tanosaki, R., Tomonaga, M., Ohashi, T., Hasegawa, A., Masuda, T., Okamura, J., Tanaka, Y., and Kannagi, M.	Potential immunogenicity of adult T cell leukemia cells in vivo	Int J Cancer	114	257-267	2005
Kannagi, M., Harashima, N., Kurihara, K., Ohashi, T., Utsunomiya, A., Tanosaki, R., Masuda, M., Tomonaga, M., and Okamura, J.	Tumor immunity against adult T-cell leukemia	Cancer Sci	96	249-255	2005

Journal of Medical Microbiology (2005), 54, 7–13 DOI 10.1099/jmm.0.45736-0

Compensatory response of IL-1 gene knockout mice after pulmonary infection with *Klebsiella pneumoniae*

Masaaki Tanabe,[1] Tetsuya Matsumoto,[1] Kazutoshi Shibuya,[2] Kazuhiro Tateda,[1] Shuichi Miyazaki,[1] Akio Nakane,[3] Yoichiro Iwakura[4] and Keizo Yamaguchi[1]

Correspondence
Tetsuya Matsumoto
tetsu@med.toho-u.ac.jp

[1,2]Department of Microbiology[1] and Department of Pathology[2], Omori Hospital, Toho University School of Medicine, 5-21-16 Omori-nishi, Ota-ku Tokyo, Japan

[3]Department of Bacteriology, Hirosaki University School of Medicine, Hirosaki, Japan

[4]Laboratory Animal Research Center, Institute of Medical Science, University of Tokyo, Tokyo, Japan

This study was designed to determine the role of interleukin (IL)-1 in the inflammatory response against experimentally induced pneumonia caused by *Klebsiella pneumoniae*. The host immune responses of IL-1 gene knockout (IL-1 KO) mice and immunocompetent wild-type (WT) mice were compared after pulmonary infection with *K. pneumoniae*. There were no significant differences between the survival rates and viable bacterial counts in lungs and blood of IL-1 KO and WT mice after pulmonary infections under different conditions. Histopathological analysis showed a similar inflammatory response in both groups of mice. However, in the early stage of infection, the level of tumour necrosis factor alpha (TNF-α) in homogenized lungs of IL-1 KO mice was significantly higher than in WT mice. To determine the role of endogenous TNF-α in the recovery of the defence mechanism in IL-1 KO mice, mice were treated with an anti-TNF-α mAb before infection with *K. pneumoniae*. The results revealed a significantly lower survival rate of anti-TNF-α mAb-treated IL-1 KO mice than BSA-treated IL-1 KO mice. The data suggest that compensatory production of TNF-α in IL-1 KO mice contributes to the host defence against *K. pneumoniae* infection.

Received 7 May 2004
Accepted 21 September 2004

INTRODUCTION

Klebsiella pneumoniae, a capsulate Gram-negative bacterium, is one of the most important causative pathogens of respiratory tract infections in humans (Podschun & Ullmann, 1998). Pneumonia caused by this organism is an expansive and voluminous pneumonia characterized by destruction of alveolar septa. This type of pneumonia is often difficult to treat, particularly in debilitated patients, with reported mortality rates of 20 to 40 % (Lawrence & Komshian, 1989; Bryan *et al.*, 1983; Edelman *et al.*, 1994; Domenico *et al.*, 1982).

Interleukin (IL)-1 is a potent proinflammatory cytokine that has been identified in numerous physiological processes as well as inflammatory diseases (Dinarello, 1996). IL-1 is an important mediator of pulmonary inflammation induced by bacteria and bacterial products (Ulich *et al.*, 1991a, b). Elevated IL-1 levels have been found in pleural fluids of patients with empyema (Silva-Mejias *et al.*, 1995) and, in patients with unilateral community-acquired pneumonia, significantly higher IL-1 concentrations have been detected in bronchoalveolar lavage fluids (BALFs) from infected lungs, compared with BALFs from non-involved lungs and serum (Dehoux *et al.*, 1994). Effective host defence against *K. pneumoniae* infection depends on a non-specific immunological response by phagocytic cells, including neutrophils and macrophages.

IL-1 and tumour necrosis factor alpha (TNF-α) are produced mainly by macrophages. IL-1 and TNF-α share a wide range of biological activities, including the activation of neutrophils (Dinarello, 1992; Ogle *et al.*, 1992; Sauder *et al.*, 1984; Shalaby *et al.*, 1985; Steinbeck & Roth, 1989). Evidence indicates that the local production of proinflammatory cytokines is crucial for clearance of bacterial infections of the lung. Indeed, passive immunization against TNF impairs host defence during pneumococcal, *Legionella* and *Klebsiella* pneumonia in mice (Brieland *et al.*, 1995; Laichalk *et al.*, 1998; van der Poll *et al.*, 1997). The role of IL-1 during *Klebsiella* pneumonia is less well defined. The present study was designed to determine the role of IL-1 in the inflammatory process after pulmonary infection with *K. pneumoniae*, by comparing the IL-1-deficient and wild-type (WT) mice.

Abbreviations: BALF, bronchoalveolar lavage fluid; KO, knockout; WT, wild-type.

METHODS

Animals. Specific pathogen-free, IL-1 gene knockout mice (IL-1 KO mice) on a BALB/c background and corresponding control BALB/c male mice were used. IL-1α/β double-gene knockout mice were produced together with mice deficient in either the IL-1α or the IL-1β genes. The IL-1 KO mice were supported at the Laboratory Animal Research Center, Institute of Medical Science, University of Tokyo. The mice were born healthy and their growth was normal (Horai *et al.*, 1998). Control WT BALB/c mice were obtained from Japan Clea Co. (Osaka, Japan). All mice were housed in a pathogen-free environment within the animal care facility at Toho University. The experimental protocol was approved by the Ethics Review Committee for Animal Experimentation of Toho University School of Medicine.

Bacteria. *K. pneumoniae* strain DT-S (capsular type 1), isolated from the sputum of a patient with pneumonia, was kindly provided by Takeda Pharmaceutical, Osaka, Japan. *K. pneumoniae* strain T-113, a clinical isolate from sputum of a patient with pneumonia, was also used. These strains were kept frozen at −80 °C in brain heart infusion (BHI) broth containing 15 % (v/v) glycerol.

Pulmonary infection with *K. pneumoniae*. Bacteria that had been cultured on blood agar for 24 h at 37 °C were suspended in sterile saline and adjusted to various densities of *K. pneumoniae*. Each mouse was anaesthetized with a mixture of xylazine, ketamine/HCl and saline by intradermal administration, followed by intranasal inoculation of 20 µl of the bacterial suspension. Survival was recorded every 24 h until 14 days after inoculation.

Determination of viable bacterial counts in blood and lung tissues. Mice were killed by ether inhalation and cardiac blood samples were collected under sterile conditions. Lungs were removed aseptically and homogenized in sterile saline using a tissue homogenizer (Omni EZ Connect Homogenizers; OMNI International). Blood and lung homogenates were serially diluted with sterile saline and added onto blood agar plates. After incubation of the medium for 24 h at 37 °C, the number of bacterial colonies was counted and the number of viable bacteria in the organs was calculated. The remaining blood samples were allowed to clot at 4 °C and then centrifuged at 14 000 *g* for 5 min. Serum samples were preserved at −80 °C until measurements of cytokines were taken.

Histopathological examination. Mice were killed at 6, 12, 24, 48 or 72 h after inoculation with *K. pneumoniae*. The lungs of mice were obtained and fixed with 4 % buffer formalin, dehydrated and embedded in paraffin. Sections were cut at 3 µm thickness and stained with haematoxylin and eosin using a standard staining procedure, then examined under a light microscope.

Determination of cytokine concentrations. The concentrations of IL-10 and IL-12, gamma interferon (IFN-γ) and TNF-α in serum and homogenized lung tissues were determined with ELISA kits purchased from Genzyme. Assays were performed according to the protocols recommended by the manufacturers.

Anti-TNF-α antibody. Hybridoma cell lines (MP6-XT22.11; rat IgG1) secreting mAb against mouse TNF-α were used. MP6-XT22.11 cells were kindly provided by J. S. Abrams, DNAX Research Institute of Cellular and Molecular Biology, Palo Alto, CA, USA. The anti-TNF-α mAbs found in the ascites fluid were partially purified by 50 % $(NH_4)_2SO_4$ precipitation (Nakane *et al.*, 1988).

Statistical analyses. Data were expressed as the mean ± standard error mean (SEM). Differences in survival rates were analysed by using the log rank test. Differences in the number of bacteria and cytokine levels were analysed by using the Mann–Whitney U-test. Differences were considered statistically significant if P values were less than 0·05.

RESULTS AND DISCUSSION

IL-1α and IL-1β are cytokines, primarily produced by activated macrophages, with central roles in the initiation and coordination of the host response to infection and injury (Dinarello, 1991). van der Meer (1988) and van der Meer *et al.* (1988) reported that pretreatment with recombinant human IL-1β (rhIL-1β) 24 h before a lethal Gram-negative infectious challenge with *K. pneumoniae* or *Pseudomonas aeruginosa* enhanced the survival of normal and neutropenic mice, respectively. We studied the effects of pulmonary administration of IL-1 before pulmonary infection with *K. pneumoniae*. The results revealed that IL-1-pretreated mice survived significantly longer than saline-pretreated control mice (T. Matsumoto, M. Tanabe, K. Yoshida, K. Tateda & K. Yamaguchi, unpublished data). These data suggest that IL-1 plays an important role in pulmonary infection with *K. pneumoniae*.

In the present study, we used IL-1 KO mice to investigate the specific role of IL-1 after pulmonary infection with *K. pneumoniae*. We evaluated the influence of IL-1 deficiency on the survival of mice after pulmonary infection with *K. pneumoniae*. The survival rates of IL-1 KO mice and WT mice were not significantly different 14 days after inoculation with *K. pneumoniae* strain T-113 ($1{\cdot}76 \times 10^2$ c.f.u. per mouse) (Fig. 1a). The use of a higher dose ($3{\cdot}6 \times 10^3$ c.f.u. per mouse) of *K. pneumoniae* strain T-113 for inoculation did not result in a significant change in the survival between the groups (Fig. 1b). We could not find any significant difference in the survival between the groups even when mice were infected with another highly virulent strain of *K. pneumoniae*, strain DT-S (at 23 c.f.u. per mouse) (Fig. 1c), and at a higher dose ($3{\cdot}6 \times 10^3$ c.f.u. per mouse) (Fig. 1d). In the preliminary study, we also evaluated the mortality rates of IL-1 KO mice and WT mice after infection with lower doses of *K. pneumoniae* strain DT-S. However, we could not find a significant difference in the mortality between these two mice strains (data not shown).

We assessed the viable number of *K. pneumoniae* in the lungs of IL-1 KO mice and WT mice at 6, 12, 24, 48 and 72 h after intranasal inoculation with *K. pneumoniae* strain DT-S. The results revealed that the number of c.f.u. in the lungs and serum was similar in the two groups at the above-mentioned times points (Fig. 2). We also evaluated the pathological changes in the lungs of WT mice and IL-1 KO mice after pulmonary infection with *K. pneumoniae*. Macropathological observation of the lungs of both WT mice and IL-1 KO mice showed severe pneumonia and similar inflammatory changes at 72 h after *K. pneumoniae* infection (Fig. 3). Viable bacterial counts in the lungs and serum showed similar kinetics in both IL-1 KO mice and WT mice. There was no apparent difference in the micropathological findings of the lungs between IL-1 KO and WT mice (Fig. 4). Inoculation with *K. pneumoniae* strain DT-S resulted in a partial

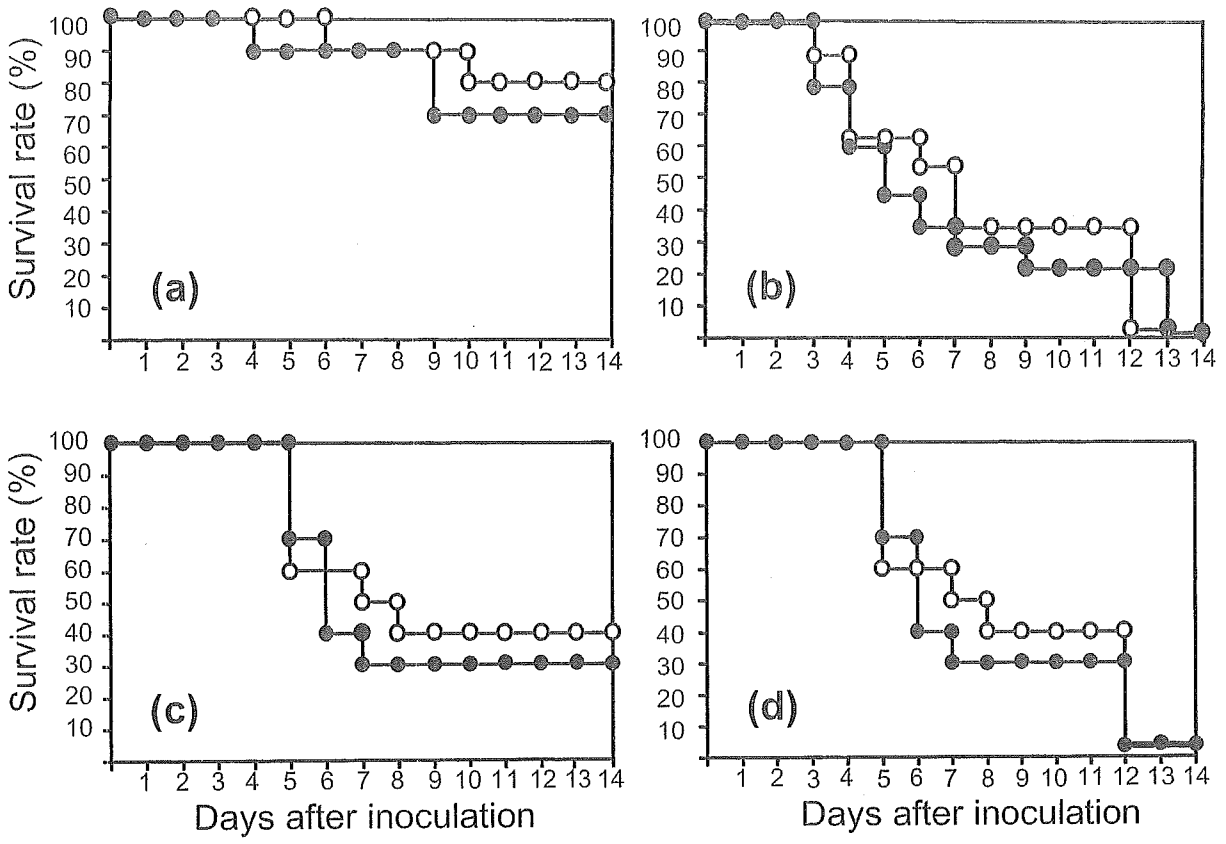

Fig. 1. Survival rates of mice after pulmonary infection caused by *K. pneumoniae*. Each mouse was inoculated intranasally with 20 µl of bacterial suspension. Inoculated bacterial doses and bacterial strains were as follows: (a) $1{\cdot}7 \times 10^2$ c.f.u. per mouse, strain T-113; (b) $3{\cdot}6 \times 10^3$ c.f.u. per mouse, strain T-113; (c) 23 c.f.u. per mouse, strain DT-S; and (d) $3{\cdot}6 \times 10^3$ c.f.u. per mouse, strain DT-S. ●, IL-1 KO mice; ○, WT mice; $n = 12$ in each group.

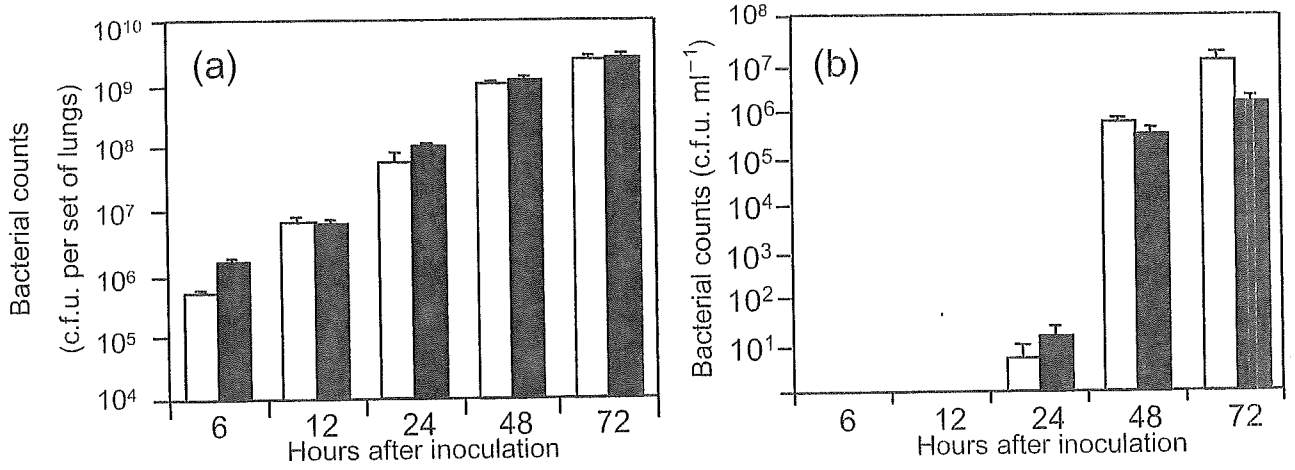

Fig. 2. Viable bacterial number in lungs (a) and in blood (b) of mice after pulmonary infection with *K. pneumoniae*. Each mouse was inoculated intranasally with $2{\cdot}0 \times 10^3$ c.f.u. of *K. pneumoniae* strain DT-S. Solid bars, IL-1 KO mice; open bars, WT mice; $n = 12$ in each group.

Fig. 3. Macroscopic findings from lungs of IL-1 KO mice and WT mice after infection with *K. pneumoniae*. Each mouse was inoculated intranasally with $2{\cdot}0 \times 10^3$ c.f.u. of *K. pneumoniae* strain DT-S. (a) Lungs of WT mice 72 h after infection with *K. pneumoniae*. (b) Lungs of IL-1 KO mice 72 h after infection with *K. pneumoniae*.

infiltration of inflammatory cells after 24 h infection. Thereafter, expansive and voluminous pneumonia characterized by the destruction of alveolar spaces was detected at 48 h after infection. Pathological findings also showed similar inflammatory responses in IL-1 KO and WT mice against pulmonary infection with *K. pneumoniae*. Although we hypothesized that IL-1 KO mice may develop more severe infection compared with WT mice after intranasal inoculation of *K. pneumoniae*, our findings suggest that IL-1 KO mice possess the same level of resistance against *K. pneumoniae* infection as present in WT mice

To determine whether deficiency of IL-1 could influence the production of other cytokines, we measured the concentrations of various cytokines in the lung homogenates of IL-1 KO mice and WT mice. The concentrations of TNF-α in the lungs of IL-1 KO mice were significantly higher than those of WT mice (Fig. 5). However, the concentrations of other cytokines (IL-10, IL-12 and IFN-γ) showed similar kinetics in these two groups (data not shown). Interestingly, TNF-α levels in the lungs of IL-1 KO mice were significantly higher than those of WT mice at 24 h after inoculation. Therefore, we think that these higher concentrations of TNF-α observed in IL-1 KO mice may assist the defence mechanism against *K. pneumoniae* pneumonia.

We studied the levels of macrophage inflammatory protein-2 (MIP-2) in the lungs 6, 12, 24, 48 and 72 h after inoculation with *K. pneumoniae*. The results suggested that there was no significant difference in the production of MIP-2 between WT mice and IL-1 KO mice (data not shown). We also evaluated the leukocyte counts in the BALFs after inoculation with *K. pneumoniae* and found that the numbers of leukocytes in the BALFs of WT mice tended to be higher than those of IL-1 KO mice at a very early time point (3 h after inoculation). However, we could not find any significant difference in the leukocyte counts in the BALFs of WT mice and IL-1 KO mice at later time points (data not shown).

Rijneveld *et al.* (2001) reported that the survival rate of IL-1 receptor type 1 gene-deficient ($R^{-/-}$) mice with *Streptococcus pneumoniae* pneumonia was not significantly different from that of WT mice. The survival rate of IL-1 $R^{-/-}$ mice pretreated with anti-TNF-α antibody was significantly lower than that of IL-1 $R^{-/-}$ mice without anti-TNF-α pretreat-

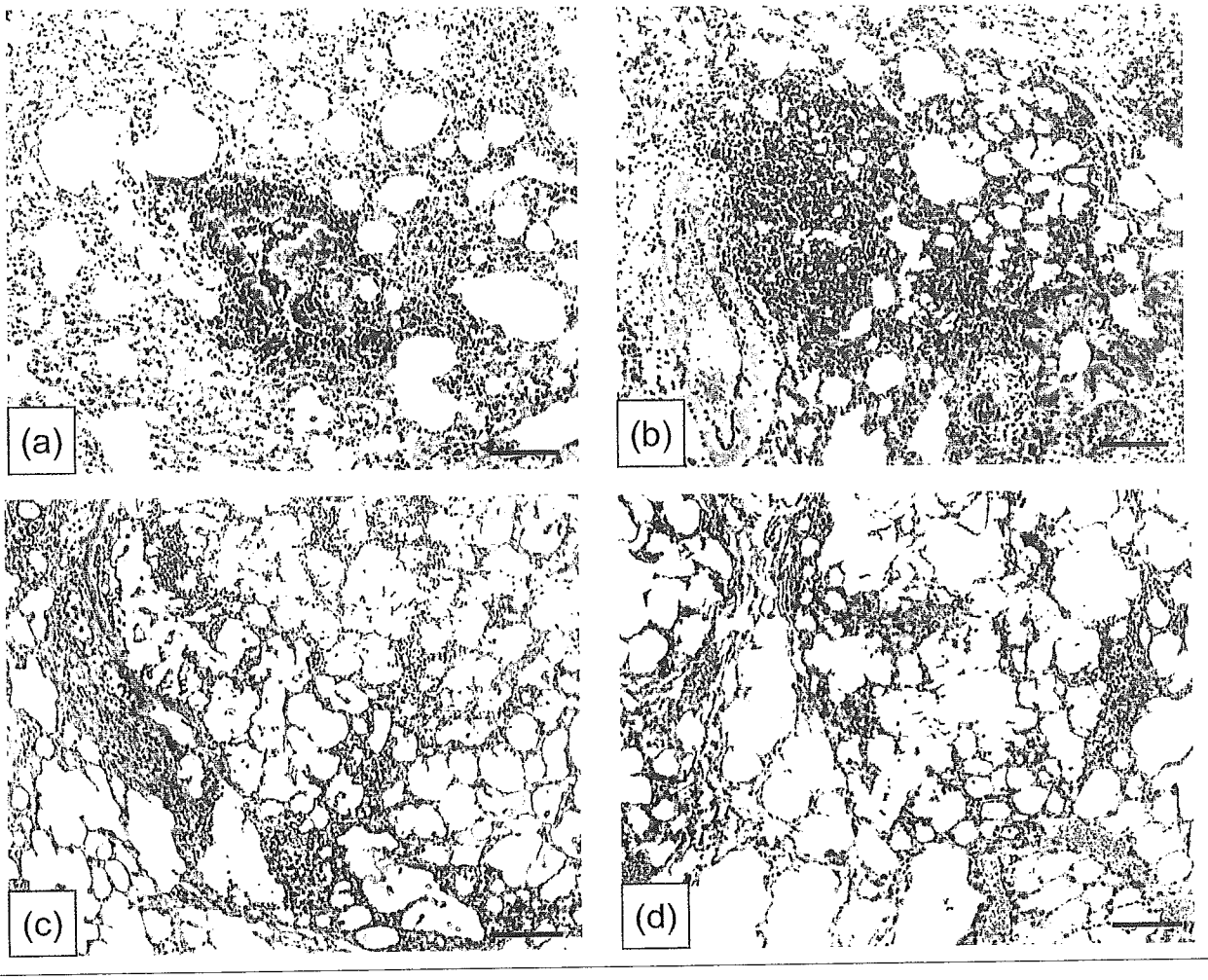

Fig. 4. Histopathological findings from lungs of IL-1 KO mice and WT mice after infection with *K. pneumoniae*. Each mouse was inoculated intranasally with $2{\cdot}0 \times 10^3$ c.f.u. of *K. pneumoniae* strain DT-S. Lungs of WT mice (a) and IL-1 KO mice (b) 24 h after inoculation with *K. pneumoniae* strain DT-S showed similar inflammatory changes, i.e. bronchopneumonia and the same level of inflammatory-cell infiltration. Lungs from WT mice (c) and IL-1 KO mice (d) 48 h after infection also showed similar histopathological findings, such as expansive and voluminous pneumonia associated with destruction of alveolar spaces. Haematoxylin and eosin stain was used; $n = 2$ in each group. Bars, 1 cm.

ment. They reported that TNF-α was more important in the defence mechanism against *S. pneumoniae* than IL-1. These studies suggested that compensatory production of TNF-α plays an important role in IL-1-deficient mice against *S. pneumoniae* pneumonia.

Laichalk *et al.* (1996) reported that administration of a TNF antagonist resulted in a significant reduction of neutrophils in BALFs, increased *K. pneumoniae* counts in BALFs and shortened the survival time of mice. On the other hand, administration of a TNF agonist resulted in a significant increase of neutrophils in BALFs, reduction of *K. pneumoniae* counts in BALFs and prolonged survival times of mice.

Since IL-1 and TNF-α can share similar proinflammatory effects *in vivo*, we determined the role of endogenous TNF-α on the defence mechanism in IL-1 KO mice by using a mAb against TNF-α. The results revealed that the survival rate of IL-1 KO mice pretreated with anti-TNF-α mAb was significantly lower than that of BSA-treated IL-1 KO mice. The survival rate of WT mice pretreated with anti-TNF-α mAb was lower than that of BSA-treated IL-1 KO mice (Fig. 6). There was no significant difference in survival between IL-1 KO and WT mice both treated with anti-TNF-α mAb, thus showing the limited role of IL-1 in the host response to *K. pneumoniae* infection and confirming the previously described results. These data suggest that TNF-α plays a more important role in the defence mechanism against *K. pneumoniae* pneumonia than IL-1.

Yamada *et al.* (2000) studied the role of IL-1 in mice infected with *Mycobacterium tuberculosis* by using the same strain of IL-1 KO mice used in the present study. They demonstrated significantly higher numbers of *M. tuberculosis* in the lungs of IL-1 KO mice than in WT mice and impaired nitric oxide production in IL-1 KO mice. Based on these data, they

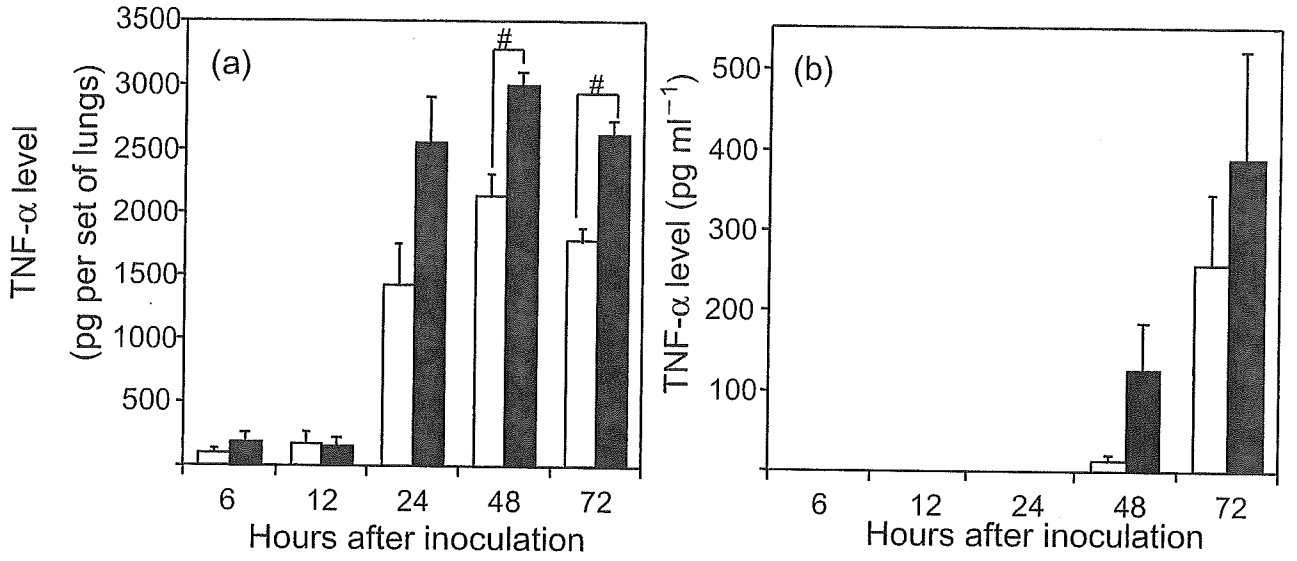

Fig. 5. TNF-α levels in the lung homogenates (a) and serum (b) of mice infected with *K. pneumoniae*. Each mouse was inoculated intranasally with $2{\cdot}0 \times 10^3$ c.f.u. of *K. pneumoniae* strain DT-S. Solid bars, IL-1 KO mice; open bars, WT mice. Data are mean ± SEM values of eight mice in each group; #, $P < 0{\cdot}05$).

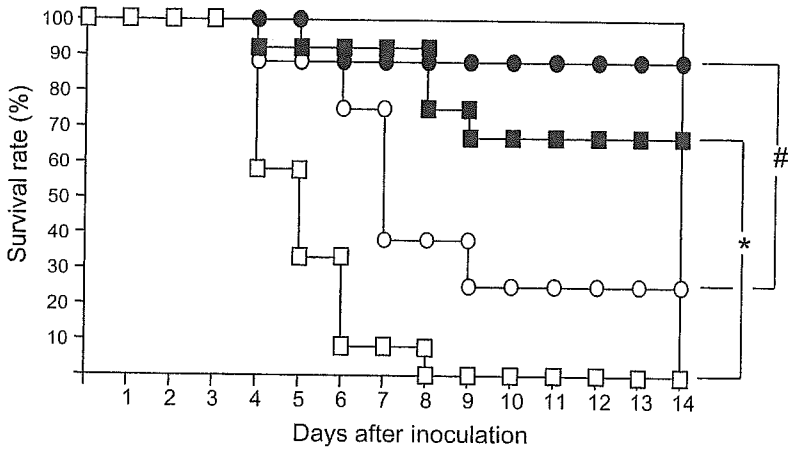

Fig. 6. Influence of antibody against TNF-α on survival rates of mice after pulmonary infection caused by *K. pneumoniae*. Each mouse was inoculated intranasally with $1{\cdot}6 \times 10^3$ c.f.u. of *K. pneumoniae* strain T-113. Mice pretreated with a neutralizing anti-mouse TNF-α mAb (−2 and 24 h; 0·2 mg; ○, WT mice; □, IL-1 KO mice) or the same concentration of BSA (●, WT mice; ■, IL-1 KO mice). #, $P < 0{\cdot}01$, WT mice vs WT mice with anti-mouse TNF-α mAb; *, $P < 0{\cdot}01$, IL-1 KO mice vs IL-1 KO mice with anti-mouse TNF-α mAb. $n = 10$ in each group.

concluded that IL-1 is important for the generation of early phase protective immunity against mycobacterial infection. However, they also pointed out that TNF-α mRNA expression was maintained within the normal range in IL-1 KO mice and suggested that TNF-α production may increase to compensate for the lack of IL-1 in IL-1 KO mice. Considered together with our results, we think that compensatory production of TNF-α in IL-1 KO mice may not always occur but that TNF-α is induced in some specific conditions, such as *K. pneumoniae* infection, as found in this study, and *P. aeruginosa* infection, as reported by Schultz *et al.* (2002).

In conclusion, our results suggest that IL-1 KO mice exhibit the same level of resistance against *K. pneumoniae* infection as WT mice. The mechanism of this phenomenon may be the compensatory enhanced production of TNF-α in IL-1 KO mice.

REFERENCES

Brieland, J. K., Remick, D. G., Freeman, P. T., Hurley, M. C., Fantone, J. C. & Engleberg, N. C. (1995). In vivo regulation of replicative *Legionella pneumophila* lung infection by endogenous tumor necrosis factor alpha and nitric oxide. *Infect Immun* **63**, 3253–3258.

Bryan, C. S., Reynolds, K. L. & Brenner, E. R. (1983). Analysis of 1,186 episodes of gram-negative bacteremia in non-university hospitals: the effects of antimicrobial therapy. *Rev Infect Dis* **5**, 629–638.

Dehoux, M. S., Boutten, A., Ostinelli, J., Seta, N., Dombret, M. C.,

Crestani, B., Deschenes, M., Trouillet, J. L. & Aubier, M. (1994). Compartmentalized cytokine production within the human lung in unilateral pneumonia. *Am J Respir Crit Care Med* **150**, 710–716.

Dinarello, C. A. (1991). Interleukin-1 and interleukin-1 antagonism. *Blood* 77, 1627–1652.

Dinarello, C. A. (1992). Role of interleukin-1 and tumor necrosis factor in systemic response to infection and inflammation. In *Inflammation: Basic Principles and Clinical Correlates*, 2nd edn, pp. 211–232. Edited by J. I. Gallin, I. M. Goldstein & R. Snyderman. New York: Raven Press.

Dinarello, C. A. (1996). Biologic basis for interleukin-1 in disease. *Blood* 87, 2095–2147.

Domenico, P., Johanson, W. G., Jr & Straus, D. C. (1982). Lobar pneumonia in rats produced by clinical isolates of *Klebsiella pneumoniae*. *Infect Immun* **37**, 327–335.

Edelman, R., Taylor, D. N., Wasserman, S. S., McClain, J. B., Cross, A. S., Sadoff, J. C., Que, J. U. & Cryz, S. J. (1994). Phase 1 trial of a 24-valent *Klebsiella* capsular polysaccharide vaccine and an eight-valent *Pseudomonas* O-polysaccharide conjugate vaccine administered simultaneously. *Vaccine* **12**, 1288–1294.

Horai, R., Asano, M., Sudo, K., Kanuka, H., Suzuki, M., Nishihara, M., Takahashi, M. & Iwakura, Y. (1998). Production of mice deficient in genes for interleukin (IL)-1α, IL-1β, IL-1α/β, and IL-1 receptor antagonist shows that IL-1β is crucial in turpentine-induced fever development and glucocorticoid secretion. *J Exp Med* **187**, 1463–1475.

Laichalk, L. L., Kunkel, S. L., Strieter, R. M., Danforth, J. M., Bailie, M. B. & Standiford, T. J. (1996). Tumor necrosis factor mediates lung antibacterial host defense in murine *Klebsiella* pneumonia. *Infect Immun* **64**, 5211–5218.

Laichalk, L. L., Bucknell, K. A., Huffnagle, G. B., Wilkowski, J. M., Moore, T. A., Romanelli, R. J. & Standiford, T. J. (1998). Intrapulmonary delivery of tumor necrosis factor agonist peptide augments host defense in murine gram-negative bacterial pneumonia. *Infect Immun* **66**, 2822–2826.

Lawrence, R. C. & Komshian, S. (1989). Gram-negative bacillary pneumonia respiratory infection. In *Diagnosis and Management*. Edited by J. E. Pennington. New York: Raven Press.

Nakane, A., Minagawa, T. & Kato, K. (1988). Endogenous tumor necrosis factor (cachectin) is essential to host resistance against *Listeria monocytogenes* infection. *Infect Immun* **56**, 2563–2569.

Ogle, J. D., Noel, J. G., Sramkoski, R. M., Ogle, C. K. & Alexander, J. W. (1992). Effects of combination of tumor necrosis factor alpha and chemotactic peptide, f-Met-Leu-Phe, on phagocytosis of opsonized microspheres by human neutrophils. *Inflammation* **16**, 57–68.

Podschun, R. & Ullmann, U. (1998). *Klebsiella* spp. as nosocomial pathogens: epidemiology, taxonomy, typing methods, and pathogenicity factors. *Clin Microbiol Rev* **11**, 589–603.

Rijneveld, A. W., Florquin, S., Branger, J., Speelman, P., Van Deventer, S. J. & van der Poll, T. (2001). TNF-alpha compensates for the impaired host defense of IL-1 type I receptor-deficient mice during pneumococcal pneumonia. *J Immunol* **167**, 5240–5246.

Sauder, D. N., Mounessa, N. L., Katz, S. I., Dinarello, C. A. & Gallin, J. I. (1984). Chemotactic cytokines: the role of leukocytic pyrogen and epidermal cell thymocyte-activating factor in neutrophil chemotaxis. *J Immunol* **132**, 828–832.

Schultz, M. J., Rijneveld, A. W., Florquin, S., Edwards, C. K., Dinarello, C. A. & van der Poll, T. (2002). Role of interleukin-1 in the pulmonary immune response during *Pseudomonas aeruginosa* pneumonia. *Am J Physiol Lung Cell Mol Physiol* **282**, L285–L290.

Shalaby, M. R., Aggarwal, B. B., Rinderknecht, E., Svedersky, L. P., Finkle, B. S. & Palladino, M. A., Jr (1985). Activation of human polymorphonuclear neutrophil functions by interferon-gamma and tumor necrosis factors. *J Immunol* **135**, 2069–2073.

Silva-Mejias, C., Gamboa-Antinolo, F., Lopez-Cortes, L. F., Cruz-Ruiz, M. & Pachon, J. (1995). Interleukin-1 beta in pleural fluids of different etiologies. Its role as inflammatory mediator in empyema. *Chest* **108**, 942–945.

Steinbeck, M. J. & Roth, J. A. (1989). Neutrophil activation by recombinant cytokines. *Rev Infect Dis* **11**, 549–568.

Ulich, T. R., Watson, L. R., Yin, S. M., Guo, K. Z., Wang, P., Thang, H. & del Castillo, J. (1991a). The intratracheal administration of endotoxin and cytokines. I. Characterization of LPS-induced IL-1 and TNF mRNA expression and the LPS-, IL-1-, and TNF-induced inflammatory infiltrate. *Am J Pathol* **138**, 1485–1496.

Ulich, T. R., Yin, S. M., Guo, K. Z., del Castillo, J., Eisenberg, S. P. & Thompson, R. C. (1991b). The intratracheal administration of endotoxin and cytokines. III. The interleukin-1 (IL-1) receptor antagonist inhibits endotoxin- and IL-1- induced acute inflammation. *Am J Pathol* **138**, 521–524.

van der Meer, J. W. (1988). The effects of recombinant interleukin-1 and recombinant tumor necrosis factor on non-specific resistance to infection. *Biotherapy* **1**, 19–25.

van der Meer, J. W., Barza, M., Wolff, S. M. & Dinarello, C. A. (1988). A low dose of recombinant interleukin 1 protects granulocytopenic mice from lethal gram-negative infection. *Proc Natl Acad Sci USA* **85**, 1620–1623.

van der Poll, T., Keogh, C. V., Buurman, W. A. & Lowry, S. F. (1997). Passive immunization against tumor necrosis factor-alpha impairs host defense during pneumococcal pneumonia in mice. *Am J Respir Crit Care Med* **155**, 603–608.

Yamada, H., Mizumo, S., Horai, R., Iwakura, Y. & Sugawara, I. (2000). Protective role of interleukin-1 in mycobacterial infection in IL-1 alpha/beta double-knockout mice. *Lab Invest* **80**, 759–767.

Immunology and Cell Biology (2005) **83**, 18–24 doi:10.1111/j.1440-1711.2005.01310.x

Research Article

IFN-γ and TNF-α are involved in urushiol-induced contact hypersensitivity in mice

TOSHITERU WAKABAYASHI,[1] DONG-LIANG HU,[1] YOH-ICHI TAGAWA,[2] KENJI SEKIKAWA,[3] YOICHIRO IWAKURA,[4] KATSUMI HANADA[5] and AKIO NAKANE[1]

[1]*Department of Bacteriology, Hirosaki University School of Medicine, Hirosaki,* [2]*Institute of Experimental Animals, Shinshu University School of Medicine, Matsumoto,* [3]*Department of Molecular Biology and Immunology, National Institute of Agrobiological Sciences, Tsukuba,* [4]*Center for Experimental Medicine, Institute of Medical Science, University of Tokyo, Tokyo and* [5]*Department of Dermatology, Hirosaki University School of Medicine, Hirosaki, Japan*

Summary Contact hypersensitivity (CHS) is a cutaneous T-cell-mediated immunological reaction to applied haptens. Activated antigen-specific T cells release several cytokines and chemokines followed by the recruitment of inflammatory cells and skin damage. $CD8^+$ T cells and $CD4^+$ T cells have been involved in the establishment of previously described CHS. In this study, we investigated the induction of CHS by urushiol in mice. Maximum swelling in mouse ears was elicited 24 h after challenge with urushiol on day 9 of sensitization. IFN-γ, TNF-α and IFN-γ-inducible protein 10 (IP-10) mRNA were expressed after challenge of the antigen in urushiol-sensitized mice, but not in unsensitized mice. IFN-γ knockout (KO) mice and TNF-α KO mice failed to elicit CHS with urushiol. Contact hypersensitivity and expressions of IFN-γ, TNF-α and IP-10 mRNA were markedly suppressed in $CD4^+$ and $CD8^+$ cell-depleted mice. These results suggest that IFN-γ, TNF-α, and possibly IP-10, play a critical role in CHS induced by urushiol, depending on both $CD4^+$ T cells and $CD8^+$ T cells.

Key words: contact hypersensitivity, IFN-γ-inducible protein 10, IFN-γ, TNF-α, urushiol.

Introduction

Contact hypersensitivity (CHS) is a cutaneous T-cell-mediated immunological reaction to applied haptens. In humans CHS manifests clinically as a pruritic dermatosis and is characterized histologically by an inflammatory mononuclear cell infiltration in the affected area. Our current understanding regarding the pathogenesis of CHS has implicated the skin as an active participant in the response. Not only does epicutaneous application of hapten result in avid binding to protein and cell membrane carriers within the skin, but epidermal Langerhans cells are also responsible for presentation of the antigen to T cells.[1] Langerhans cells migrate to the regional lymph nodes and initiate a primary immune response to the hapten in a MHC-restricted manner. Subsequent contact or challenge with the hapten results in cutaneous infiltration of the primed T cells and activated antigen-specific T cells release several cytokines and chemokines followed by the recruitment of inflammatory cells and local tissue damage.[1] Although both clinical and experimental studies have suggested that $CD4^+$ and $CD8^+$ T cells act as the effector T cells mediating CHS,[2,3] a number of studies have indicated that $CD8^+$ T cells act as effector cells in CHS responses in mice and that $CD4^+$ T cells regulate the magnitude of CHS.[4,5]

Correspondence: Akio Nakane, Department of Bacteriology, Hirosaki University School of Medicine, 5 Zaifu-cho, Hirosaki, Aomori 036-8562, Japan. Email: a27k03n0@cc.hirosaki-u.ac.jp

Received 22 March 2004; accepted 7 September 2004.

$CD4^+$ T cells and $CD8^+$ T cells are induced and differentiate into distinct functional subsets, type 1 (Th1 or T-cytotoxic 1 [Tc1]) and type 2 (Th2 or Tc2). Type 1 cells secrete IL-2 and IFN-γ, whereas type 2 cells secrete IL-4, IL-5, IL-10 and IL-13.[6,7] It is generally recognized that type 1 cytokines play an effector role in CHS, whereas type 2 cytokines play a regulatory role. The effector role of IFN-γ in CHS was confirmed by the demonstration of an impaired FITC-induced CHS response in IFN-γ receptor 2 deficient mice.[8] However, 2,4-dinitrofluorobenzene (DNFB)-induced CHS responses are reportedly normal in IFN-γ deficient mice.[9] Pro-inflammatory cytokines, such as TNF-α, are also involved in CHS. Anti-TNF-α mAb treatment suppressed 2,4,6-trinitro-1-chlorobenzene (TNCB)-induced CHS more powerfully than anti-IFN-γ mAb treatment.[10] CHS was not induced in TNF-α deficient mice and TNF-α receptor 2 deficient mice, which suggests that TNF-α plays an important role in CHS induction.[11]

There have been numerous studies examining hapten-induced CHS using DNFB, TNCB and oxazolone. However, these are artificial compounds and it is unlikely that we will come into contact with these compounds in our daily life. Members of *Anacardiaceae*, including poison ivy, poison oak and poison sumac plants, produce oil that can cause contact sensitivity in humans and animals. The debilitating dermatitis resulting from contact with these plants represents a severe hazard for outdoor workers. Oils extracted from these plants are closely related chemically and are called urushiols.[12] They are composed of mixtures of 3-*n*-alk(en)ylcatechols in which the side chains consist of either a C-15 or a C-17 moiety.[13,14]

Although the implication of $CD4^+$ T cells and $CD8^+$ T cells in CHS induced by urushiol has been demonstrated in human peripheral blood *in vitro* and in mice *in vivo*,[15,16] the roles of cytokines such as IFN-γ and TNF-α in urushiol-induced CHS have not been assessed. Thus, we were interested in the implication of cytokines in a mouse CHS model using urushiol. In this study we demonstrate that IFN-γ and TNF-α play a critical role in the induction of CHS induced by urushiol and that the induction of CHS is dependent on $CD4^+$ cells and $CD8^+$ cells.

Materials and methods

Mice

Male and female C57BL/6 mice, IFN-γ knockout (KO) mice and TNF-α KO mice on a C57BL/6 × Sv129 background[17,18] and aged 6–8 weeks old were used. C57BL/6 mice were obtained from Japan SLC (Hamamatsu, Shizuoka, Japan). All animals were maintained under specific pathogen-free conditions at the Institute for Animal Experiments, Hirosaki University School of Medicine. All animal experiments were carried out in accordance with the Guidelines for Animal Experimentation of Hirosaki University.

Allergen

Urushiol isolated from *Rhus verniciflua*, the urushi tree, was kindly supplied by Torii Pharmaceutical (Tokyo, Japan). Urushiol was dissolved in acetone/olive oil (A/O) at a ratio of 4:1.

Anti-TNF-α monoclonal antibody treatment

A hybridoma cell line secreting a mAb against mouse TNF-α (MP6-XT22.11, rat IgG_1) was used.[19] The mAb found in the ascites fluid was partially purified using $(NH_4)_2SO_4$ precipitation. Mice were given a single intraperitoneal injection of 1 mg of the mAb 1 h before sensitization with urushiol. Isotype-matched IgG_1 was injected as a control.

Monoclonal antibodies against cell surface molecules

Mice were injected intraperitoneally with a single 400 μg dose of mAb against mouse CD4 (GK1.5, rat IgG_{2b}) and mouse CD8 (53–6.72, rat IgG_{2a}) 3 days before sensitization. Using these schedules and doses, we confirmed that anti-CD4 mAb could deplete more than 90% of $CD4^+$ cells in the spleens and mesenteric lymph nodes for at least 10 days and that anti-CD8 mAb could deplete more than 90% of $CD8^+$ cells in the organs for at least 17 days.[20] Isotype-matched IgG was injected as a control.

Induction of CHS by urushiol

Mice were sensitized with 30 μL of 20 mg/mL urushiol in A/O on shaved abdominal skin on day 0 and challenged with 15 μL of 10 mg/mL urushiol in A/O on both surfaces of each ear on day 9. Ear thickness was measured with a digimatic micrometer (Mitsutoyo, Kanagawa, Japan) just prior to and 24 h after challenge.

Histological evaluation

Skin samples from the ears were collected from C57BL/6 mice, IFN-γ KO mice and TNF-α KO mice 24 h after challenge. These specimens were embedded in paraffin for histological staining using haematoxylin and eosin.

Real-time quantitative PCR

Total RNA was isolated from pieces of spleen and liver (0.05 g each) using a guanidium–thiocyanate–phenol–chloroform single-step method. First-strand cDNA were synthesized using reverse transcription of 1 μg total RNA with random primers (Takara, Shiga, Japan) and reverse transcriptase Moloney murine leukaemia virus (Invitrogen, Carlsbad, CA, USA). The following primers were used for IFN-γ, forward 5′-AGCGGCTGACTGAACTCAGATTGTAG-3′ and reverse 5′-GTCACAGTTTTCAGCTGTATAGGG-3′; for TNF-α, forward 5′-GGCAGGTCTACTTTGGAGTCATTGC-3′ and reverse 5′-ACATTCGAGGCTCCAGTGAATTCGG-3′; for IFN-γ-inducible protein 10 (IP-10), forward 5′-TGTTCTGGTGACAAGCTC CTG-3′ and reverse 5′-GCCAAATTTAGCCAGATCCA-3′; and for glyceraldehyde 3-phosphate dehydrogenase (GAPDH), forward 5′-TGAAGGTCGGTGTGAACGGATTTGG-3′ and reverse 5′-ACGACATACTCAGCACCAGCATCAC-3′. SYBER Green Supermix (Bio-Rad, Hercules, CA, USA) was used as a PCR reaction solution. The following protocol was used to run the PCR: initial activation of AmpliTaq Gold DNA polymerase at 95°C for 3 min, 30 s (IFN-γ, GAPDH and TNF-α) or 1 min (IP-10) at 94°C for denaturing, 30 s at 55°C (IFN-γ and GAPDH) or 62°C (TNF-α) or 1 min (IP-10) at 58°C for annealing, 3 min at 72°C for elongation and 50 PCR cycles were carried out. All experiments were run in duplicate and non-template controls and dissociation curves were used to detect primer–dimer conformation and non-specific amplification. The threshold cycle (C_T) of each target product was determined and set in relation to the amplification plot of GAPDH. The detection threshold is set to the log linear range of the amplification curve and was kept constant (0.05) for all data analyses. The difference in the C_T values (ΔC_T) of two genes was used to calculate the fold difference [fold difference = $2^{-(C_T \text{ of cytokine} - C_T \text{ of GADPH})} = 2^{-\Delta C_T}$].[21]

Statistical evaluation of the data

Data were expressed as mean ± SD and Student's *t*-tests were used to determine significant differences in ear swelling between the control and experimental groups. *P*-values of <0.05 were considered to be statistically significant.

Results

Induction of CHS by urushiol

Mice were sensitized on shaved abdominal skin with 30 μL of 20 mg/mL urushiol on day 0 and challenged on both surfaces of each ear with 15 μL of 10 mg/mL urushiol on days 4–10. Ear thickness was measured just prior to and 24 h after challenge. Ear swelling peaked 9 days after sensitization (Fig. 1a). We also assessed the time point of maximal ear swelling after challenge and ear swelling reached its peak 24 h after challenge (Fig. 1b). In addition, we examined the effect of different doses of urushiol on CHS. Mice were sensitized with various concentrations of urushiol and challenged with different doses of urushiol on day 9. Ear swelling was maximal when mice were sensitized with 20 mg/mL urushiol and challenged with 10 mg/mL urushiol (Fig. 1c). In contrast, there was no difference in the degree of ear swelling in unsensitized mice between the unchallenged and challenged groups (data not shown).

Local expression of cytokines in mouse ears after challenge

IFN-γ can stimulate keratinocytes to produce IP-10.[22] Therefore, we examined IP-10 mRNA expression in addition to

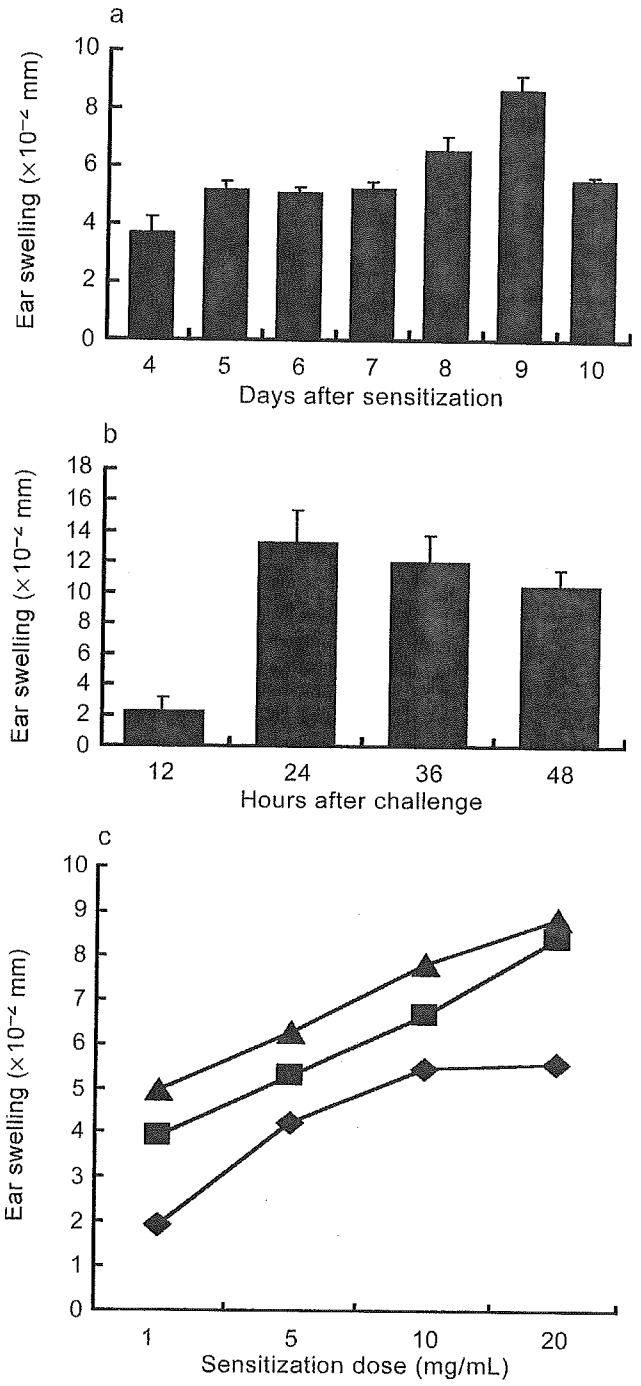

Figure 1 Induction of contact hypersensitivity (CHS) by urushiol. (a) C57BL/6 mice were sensitized with 30 μL of 20 mg/mL urushiol and challenged with 15 μL of 10 mg/mL urushiol on both surfaces of each ear on days 4–10. Ear thickness was measured with a digimatic micrometer just prior to and 24 h after challenge. (b) C57BL/6 mice were sensitized with 30 μL of 20 mg/mL urushiol and challenged with 15 μL of 10 mg/mL urushiol on both surfaces of each ear on day 9. Ear thickness was measured just prior to and 12, 24, 36 and 48 h after challenge. (c) C57BL/6 mice were sensitized on shaved abdominal skin with 30 μL of 20, 10, 5 or 1 mg/mL urushiol on day 0. They were challenged on both surfaces of each ear with 15 μL of 10 (▲), 5 (■), or 1 (◆) mg/mL of urushiol on day 9. Ear thickness was measured just prior to and 24 h after challenge. Each result represents the mean ± SD for a group of four mice.

expressions of IFN-γ and TNF-α mRNA in the ears of sensitized mice after challenge. Ear samples were collected 12 h after challenge and the expressions of IFN-γ, TNF-α and IP-10 mRNA were assessed using real-time quantitative PCR. Mice that were sensitized and challenged with urushiol revealed high expressions of IFN-γ, TNF-α and IP-10 compared with unsensitized and challenged mice (Table 1).

Role of IFN-γ and TNF-α in CHS induced by urushiol

We confirmed the production of IFN-γ, TNF-α and IP-10 in ear specimens of urushiol-sensitized mice after challenge. Thus, the next step was to examine the implication of IFN-γ and TNF-α in CHS induced by urushiol. C57BL/6 mice, IFN-γ KO mice and TNF-α KO mice were sensitized with urushiol and challenged with urushiol 9 days later. Enhanced ear swelling was observed in urushiol-sensitized mice compared with unsensitized mice. In contrast, no ear swelling was evoked in IFN-γ KO mice or in TNF-α KO mice (Fig. 2). Next, we compared the histology of ears obtained from C57BL/6 mice, IFN-γ KO mice and TNF-α KO mice 24 h after challenge. The CHS in C57BL/6 mice showed dermal oedema and infiltration by inflammatory mononuclear cells (Fig. 3a). In contrast, there was no dermal oedema in IFN-γ KO mice or in TNF-α KO mice (Fig. 3b,c). Defective organization of peripheral lymphoid organs, including failure of germinal centre formation, was observed in TNF-α KO mice.[17] To exclude the architectural effect of TNF-α KO mice, we examined the induction of CHS by urushiol in anti-TNF-α mAb-treated mice. Injection of anti-TNF-α mAb into C57BL/6 mice before sensitization with urushiol significantly suppressed ear swelling after challenge (anti-TNF-α mAb-treated mice, 0.055 ± 0.006 mm; control IgG-treated mice, 0.095 ± 0.005 mm; $n = 5$, $P < 0.01$).

Effect of in vivo *depletion of T cells on CHS induced by urushiol*

We assessed the implication of T cells in IFN-γ, TNF-α and IP-10 production. Mice were injected with anti-CD4 mAb, anti-CD8 mAb or isotype-matched control IgG 3 days before sensitization. Ear swelling was completely inhibited in both $CD4^+$ T-cell-depleted and $CD8^+$ T-cell-depleted mice (Fig. 4). We also examined the local expression of IFN-γ, TNF-α and IP-10 mRNA in these mice 12 h after challenge. The levels of IFN-γ and IP-10 mRNA expression were lower than those in isotype-matched control IgG-treated mice (Table 2) and TNF-α mRNA was not detected in these specimens (data not shown). Subsequently, we compared the histology of ears obtained from $CD4^+$ T-cell-depleted mice, $CD8^+$ T-cell-depleted mice and control IgG-treated mice 24 h after challenge. The CHS in control IgG-treated mice showed dermal oedema and infiltration by inflammatory mononuclear cells (Fig. 5a). In contrast, there was no dermal oedema in $CD4^+$ T-cell-depleted mice or $CD8^+$ T-cell-depleted mice (Fig. 5b,c).

Discussion

Although there have been a number of reports examining CHS induced by urushiol, most of these studies have dealt with tolerance to CHS induced by urushiol.[16,23,24] In the

Table 1 Expressions of cytokines in ear specimens after challenge with urushiol

Sensitized with urushiol	Challenged with urushiol	Cytokine mRNA expression (fold difference)
No	Yes	IFN-γ (0.18 ± 0.23)
Yes	Yes	($\times 10^{-2}$) (76.86 ± 21.72)
No	Yes	TNF-α (9.75 ± 8.42)
Yes	Yes	($\times\#10^{-5}$) (84.32 ± 30.53)
No	Yes	IP-10 (5.50 ± 2.10)
Yes	Yes	($\times 10^{-4}$) (12.79 ± 8.34)

C57BL/6 mice were sensitized on shaved abdominal skin with 30 μL of 20 mg/mL urushiol on day 0. They were challenged on both surfaces of each ear with 15 μL of 10 mg/mL urushiol on day 9. Ear samples were collected 12 h after challenge and cytokine mRNA expression was assessed using real-time quantitative PCR. Each result represents the mean ± SD for a group of 12 mice from three experiments.

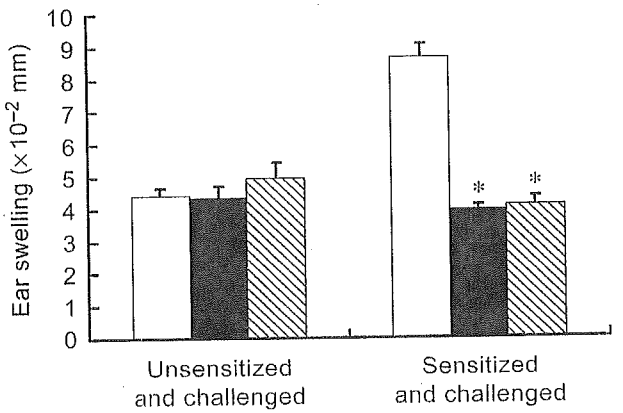

Figure 2 The role of IFN-γ and TNF-α in contact hypersensitivity (CHS) induced by urushiol. C57BL/6 mice (□), IFN-γ knockout (KO) mice (■) and TNF-α KO mice (▨) were sensitized on shaved abdominal skin with 30 μL of 20 mg/mL urushiol on day 0 and challenged on both surfaces of each ear with 15 μL of 10 mg/mL urushiol on day 9. Unsensitized mice were also challenged with urushiol. Ear thickness was measured with a digimatic micrometer just prior to and 24 h after challenge. Each point represents the mean ± SD for a group of six mice. An asterisk indicates that the value is significantly different from the value obtained from the sensitized and challenged C57BL/6 mice ($P < 0.01$).

present study, we investigated the mechanism of the induction of CHS by urushiol in mice. Our results showed that the peak intensity of ear swelling was observed 9 days after sensitization and 24 h after challenge, depending on urushiol concentrations (Fig. 1). Contact hypersensitivity is histologically characterized by dermal oedema and inflammatory mononuclear cell infiltration in the affected area.[16,25] In this study, dermal oedema and inflammatory mononuclear cell infiltration were recognized in sensitized and challenged C57BL/6 mice (Fig. 3a), indicating that we could establish a mouse CHS model using urushiol.

IFN-γ is a predominant cytokine during antigen presentation[26] and TNF-α plays an important role in CHS induction.[11] IFN-γ can stimulate keratinocytes to produce IP-10.[22] The recruitment of lymphocytes into inflamed skin is a multi-step process involving recognition of vascular endothelial cells and extravasation. Haptens can rapidly induce expression of E-selectins and P-selectins and vascular cell adhesion

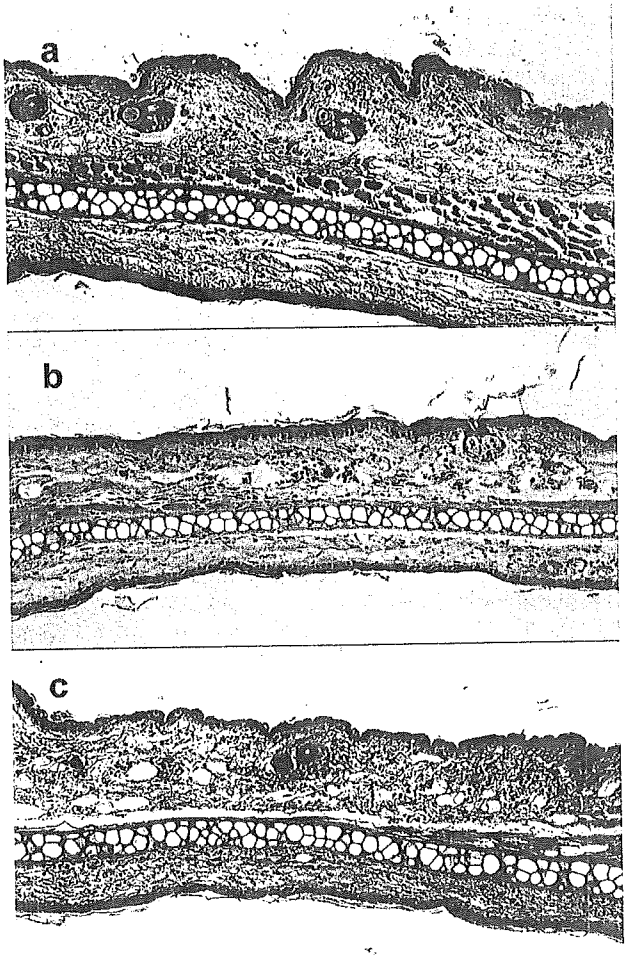

Figure 3 Histological evaluation of contact hypersensitivity (CHS) induced by urushiol in (a) C57BL/6 mice, (b) IFN-γ knockout (KO) mice and (c) TNF-α KO mice. Skin samples of ears were collected 24 h after challenge. These specimens were embedded in paraffin for histological staining with haematoxylin and eosin. Magnification ×200.

molecule-1 (VCAM-1) and intercellular adhesion molecule-1 (ICAM-1) on endothelial cells.[27,28] Several reports have shown that there was marked oedema resulting from the local release of TNF-α, serotonin and histamine from mast cells and platelets 2 h after topical application of antigen to the ears

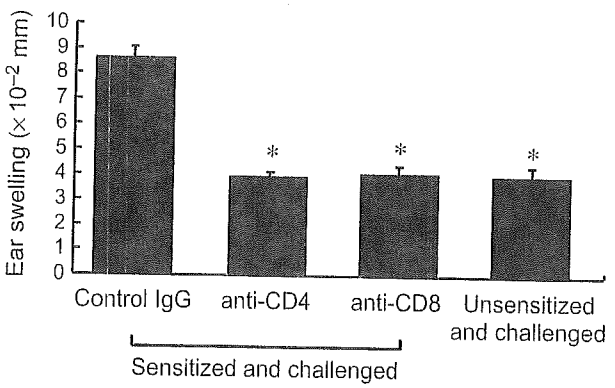

Figure 4 Effects of *in vivo* depletion of T cells on ear swelling induced by urushiol. Mice were injected intraperitoneally with a single 400 μg dose of mAb against mouse CD4 or mouse CD8 3 days before sensitization. Ear thickness was measured with a digimatic micrometer just prior to and 24 h after challenge. Each point represents the mean ± SD for a group of six mice. An asterisk indicates that the value is significantly different from the value obtained from the control IgG-treated mice ($P < 0.01$).

Table 2 Expressions of cytokines in ear specimens of T-cell subset-depleted mice

Treatment	Cytokine mRNA expression (× 10^{-3} fold difference)
Control IgG	IFN-γ (46.31 ± 34.02)
Anti-CD4	IFN-γ (2.12 ± 1.91)
Anti-CD8	IFN-γ (2.64 ± 1.39)
Control IgG	IP-10 (1.74 ± 1.17)
Anti-CD4	IP-10 (0.10 ± 0.08)
Anti-CD8	IL-10 (0.26 ± 0.14)

C57BL/6 mice were injected intraperitoneally with a single 400 μg dose of mAb against mouse CD4 or mouse CD8 3 days before sensitization. Ear samples were collected 12 h after challenge and cytokine mRNA expression was assessed using real-time quantitative PCR. Each result represents the mean ± SD for a group of 12 mice from three experiments.

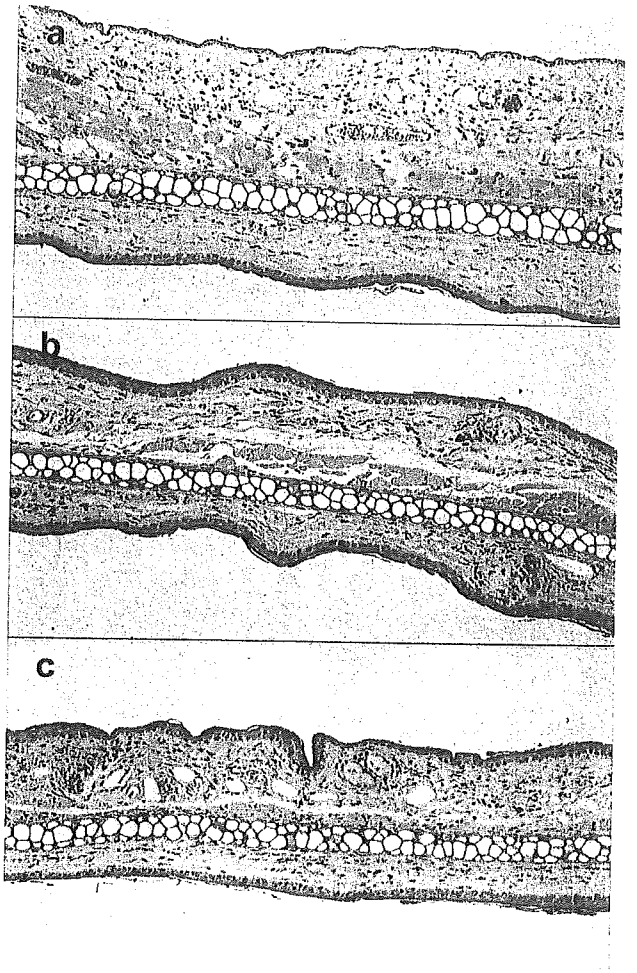

Figure 5 Histological evaluation of contact hypersensitivity (CHS) to urushiol in $CD4^+$-cell-depleted mice and $CD8^+$-cell-depleted mice. Skin samples of ears were collected 24 h after challenge. These specimens were embedded in paraffin for histological staining with haematoxylin and eosin. Magnification ×200.

of sensitized mice.[10,29] An early release of TNF-α induced expression of VCAM-1 and ICAM-1 on the luminal surface of local endothelium. These adhesion molecules mediate rolling, adhesion and extravasation of blood leucocytes expressing cutaneous lymphocyte-associated antigen or P-selectin ligands into the skin.[28] In the present study, the expression of IFN-γ, TNF-α and IP-10 mRNA was upregulated in sensitized and challenged mice compared with unsensitized mice (Table 1), although TNF-α reportedly plays an important role in the induction of CHS by haptens.[10,11] Inconsistent results have been reported with regard to the role of IFN-γ in CHS induced by haptens.[8,9,11] Our results demonstrated that no ear swelling was elicited in IFN-γ KO mice and in TNF-α KO mice (Fig. 2) and that there was no dermal oedema in these cytokine-deficient mice (Fig. 3). These results suggest that IFN-γ and TNF-α, and possibly IP-10, play an important role in the development of CHS induced by urushiol.

CD4 and CD8 molecules are two key co-receptors on T cells that stabilize and increase the avidity of the interaction between the T-cell receptor and peptide MHC determinants on APC. Previous studies have indicated that $CD8^+$ T cells are the effector cells and that $CD4^+$ T cells regulate the magnitude of CHS.[4,5] Our present results indicated that ear swelling and CHS-like histological features were not observed and the expressions of IFN-γ, TNF-α and IP-10 mRNA were suppressed in $CD4^+$ cell-depleted and $CD8^+$ cell-depleted mice (Figs 4,5; Table 2). IFN-γ-producing $CD8^+$ T cells play a crucial role in the elicitation of CHS induced by DNFB or TNCB.[4,5,30,31] Expression of IP-10 is induced by $CD8^+$ T cells most likely via IFN-γ[32] and cultured human keratinocytes have been shown to produce IP-10 by stimulation with IFN-γ or TNF-α.[33] TNF-α is known to be produced by $CD4^+$ T cells and macrophages. $CD8^+$ T cells are reportedly major TNF-α-producing cells in acquired immunity to intracellular-growing pathogens such as *Listeria monocytogenes*.[34] Our results suggest that both $CD4^+$ T cells and $CD8^+$ T cells contribute to the development of urushiol-induced CHS and that IFN-γ, TNF-α and IP-10 production may be dependent on both T-cell subsets. Alternatively, it is possible that $CD8\alpha^+$ dendritic cells are also involved in the production of these cytokines.[35]

The development of this system will allow studies to examine important aspects of the mechanism of CHS induced by *Anacardiaceae*. Pistachio nuts, cashew nuts, mangoes and rhus belong to the *Anacardiaceae* family,[36] and mango dermatitis is famous as a severe symptom. Further understanding of the mechanism for urushiol-induced CHS may lead to treatment with new methods or to the prevention of CHS induced by *Anacardiaceae*.

References

1 Friedmann PS. Contact hypersensitivity. *Curr. Opin. Immunol.* 1989; **1**: 690–3.

2 Cavani A, Albanesi C, Traidl C, Sebastiani S, Girolomoni G. Effector and regulatory T cells in allergic contact dermatitis. *Trends Immunol.* 2001; **22**: 118–20.

3 Wang B, Feliciani C, Freed I, Cai Q, Sauder DN. Insights into molecular mechanisms of contact hypersensitivity gained from gene knockout studies. *J. Leukoc. Biol.* 2001; **70**: 185–91.

4 Kehren J, Desvignes C, Krasteva M *et al.* Cytotoxicity is mandatory for CD8(+) T cell-mediated contact hypersensitivity. *J. Exp. Med.* 1999; **189**: 779–86.

5 Martin S, Lappin MB, Kohler J *et al.* Peptide immunization indicates that $CD8^+$ T cells are the dominant effector cells in trinitrophenyl-specific contact hypersensitivity. *J. Invest. Dermatol.* 2000; **115**: 260–6.

6 Sad S, Marcotte R, Mosmann TR. Cytokine-induced differentiation of precursor mouse $CD8^+$ cells secreting TH1 or TH2 cytokines. *Immunity* 1995; **2**: 271–9.

7 Abbas AK, Murphy KM, Sher A. Functional diversity of helper T lymphocytes. *Nature* 1996; **383**: 789–93.

8 Lu B, Ebensperger C, Dembic Z *et al.* Targeted disruption of the interferon-γ receptor 2 gene results in severe immune defects in mice. *Proc. Natl Acad. Sci. USA* 1998; **95**: 8233–8.

9 Reeve VE, Bosnic M, Nishimura N. Interferon-γ is involved in photoimmunoprotection by UVA (320–400 nm) radiation in mice. *J. Invest. Dermatol.* 1999; **112**: 945–50.

10 Piguet PF, Grau GE, Hauser C, Vassalli P. Tumor necrosis factor is a critical mediator in hapten induced irritant and contact hypersensitivity reactions. *J. Exp. Med.* 1991; **173**: 673–9.

11 Biedermann T, Kneilling M, Mailhammer R *et al.* Mast cells control neutrophil recruitment during T cell-mediated delayed-type hypersensitivity reactions through tumor necrosis factor and macrophage inflammatory protein 2. *J. Exp. Med.* 2000; **192**: 1441–52.

12 Kigman AM. Poison ivy (*Rhus*) dermatitis. *Arch. Dermatol.* 1958; **77**: 149–80.

13 Symes WF, Dawson CR. Poison ivy 'urushiol'. *J. Am. Chem. Soc.* 1975; **76**: 2959–63.

14 Billets SJ, Craig JC, Corbett MD, Vickery JF. Component analysis of the urushiol content of poison ivy and poison oak. *Phytochemistry* 1976; **15**: 533–5.

15 Kalish RS, Wood JA, LaPorte A. Processing of urushiol (poison ivy) hapten by both endogenous and exogenous pathways for presentation to T cells in vitro. *J. Clin. Invest.* 1994; **93**: 2039–47.

16 Lopez CB, Kalergis AM, Becker MI, Garbarino JA, De Ioannes AE. $CD8^+$ T cells are the effectors of the contact dermatitis induced by urushiol in mice and are regulated by $CD4^+$ T cells. *Int. Arch. Allergy Immunol.* 1998; **117**: 194–201.

17 Taniguchi T, Takata M, Ikeda A, Momotani E, Sekikawa K. Failure of germinal center formation and impairment of response to endotoxin in tumor necrosis factor alpha-deficient mice. *Lab. Invest.* 1997; **77**: 647–58.

18 Tagawa Y, Sekikawa K, Iwakura Y. Suppression of concanavalin A-induced hepatitis in IFN-$\gamma^{-/-}$ mice, but not in TNF-$\alpha^{-/-}$ mice: role for IFN-γ in activating apoptosis of hepatocytes. *J. Immunol.* 1997; **159**: 1418–28.

19 Nakane A, Yamada K, Hasegawa S *et al.* Endogenous cytokines during a lethal infection with *Listeria monocytogenes* in mice. *FEMS Microbiol. Lett.* 1999; **175**: 133–42.

20 Nakane A, Numata A, Chen Y, Minagawa T. Endogenous gamma interferon-independent host resistance against *Listeria monocytogenes* infection in $CD4^+$ T cell- and asialo $GM1^+$ cell-depleted mice. *Infect. Immun.* 1991; **59**: 3439–45.

21 Ishida Y, Kondo T, Ohshima T, Fujiwara H, Iwakura Y, Mukaida N. A pivotal involvement of IFN-γ in the pathogenesis of acetaminophen-induced acute liver injury. *FASEB J.* 2002; **16**: 1227–36.

22 Nakae S, Komiyama Y, Narumi S *et al.* IL-1-induced tumor necrosis factor-α elicits inflammatory cell infiltration in the skin by inducing IFN-γ-inducible protein 10 in the elicitation phase of the contact hypersensitivity response. *Int. Immunol.* 2003; **15**: 251–60.

23 Ikeda Y, Yasuno H, Sato A, Kawai K. Oral and epicutaneous desensitization in urushiol contact dermatitis in guinea pigs sensitized by 2 methods of different sensitizing potency. *Contact Dermatitis* 1998; **39**: 286–92.

24 Kalish RS, Wood JA. Induction of hapten-specific tolerance of human $CD8^+$ urushiol (poison ivy)-reactive T lymphocytes. *J. Invest. Dermatol.* 1997; **108**: 253–7.

25 McMillan EM, Stoneking L, Burdick S, Cowan I, Husain-Hamzavi SL. Immunophenotype of lymphoid cells in positive patch tests of allergic contact dermatitis. *J. Invest. Dermatol.* 1985; **84**: 229–33.

26 Boehm U, Klamp T, Groot M, Howard JC. Cellular responses to interferon-γ. *Annu. Rev. Immunol.* 1997; **15**: 749–95.

27 Goebeler M, Meinardus-Hager G, Roth J, Goerdt S, Sorg C. Nickel chloride and cobalt chloride, two common contact sensitizers, directly induce expression of intercellular adhesion molecule-1 (ICAM-1), vascular cell adhesion molecule-1 (VCAM-1), and endothelial leukocyte adhesion molecule (ELAM-1) by endothelial cells. *J. Invest. Dermatol.* 1993; **100**: 759–65.

28 McHale JF, Harari OA, Marshall D, Haskard DO. Vascular endothelial cell expression of ICAM-1 and VCAM-1 at the onset of eliciting contact hypersensitivity in mice: evidence for a dominant role of TNF-α. *J. Immunol.* 1999; **162**: 1648–55.

29 Matsuda H, Ushio H, Geba GP, Askenase PW. Human platelets can initiate T cell-dependent contact sensitivity through local serotonin release mediated by IgE antibodies. *J. Immunol.* 1997; **158**: 2891–7.

30 Okazaki F, Kanzaki H, Fujii K *et al.* Initial recruitment of interferon-γ-producing CD8+ effector cells, followed by infiltration of CD4+ cells in 2,4,6-trinitro-1-chlorobenzene (TNCB)-induced murine contact hypersensitivity reactions. *J. Dermatol.* 2002; **29**: 699–708.

31 Wang B, Fujisawa H, Zhuang L *et al.* CD4+ Th1 and CD8+ type 1 cytotoxic T cells both play a crucial role in the full development of contact hypersensitivity. *J. Immunol.* 2000; **165**: 6783–90.

32 Abe M, Kondo T, Xu H, Fairchild RL. Interferon-γ inducible protein (IP-10) expression is mediated by CD8+ T cells and is regulated by CD4+ T cells during the elicitation of contact hypersensitivity. *J. Invest. Dermatol.* 1996; **107**: 360–6.

33 Boorsma DM, de Haan P, Willemze R, Stoof TJ. Human growth factor (huGRO), interleukin-8 (IL-8) and interferon-γ-inducible protein (γ-IP-10) gene expression in cultured normal human keratinocytes. *Arch. Dermatol. Res.* 1994; **286**: 471–5.

34 Wong P, Pamer EG. CD8 T cell responses to infectious pathogens. *Annu. Rev. Immunol.* 2003; **21**: 29–70.
35 Ardavin C. Origin, precursors and differentiation of mouse dendritic cells. *Nat. Rev. Immunol.* 2003; **3**: 582–90.
36 Powell SM, Barrett DK. An outbreak of contact dermatitis from Rhus verniciflua (Toxicodendron vernicifluum). *Contact Dermatitis* 1986; **14**: 288–9.

Overexpression of the Runx3 Transcription Factor Increases the Proportion of Mature Thymocytes of the CD8 Single-Positive Lineage[1]

Kazuyoshi Kohu,* Takehito Sato,[§] Shin-ichiro Ohno,[§] Keitaro Hayashi,* Ryuji Uchino,* Natsumi Abe,* Megumi Nakazato,* Naomi Yoshida,* Toshiaki Kikuchi,[†] Yoichiro Iwakura,[¶] Yoshihiro Inoue,[‡] Toshio Watanabe,* Sonoko Habu,[§] and Masanobu Satake[2]*

The Runx family of transcription factors is thought to regulate the differentiation of thymocytes. Runx3 protein is detected mainly in the $CD4^-8^+$ subset of T lymphocytes. In the thymus of *Runx3*-deficient mice, *CD4* expression is de-repressed and $CD4^-8^+$ thymocytes do not develop. This clearly implicates Runx3 in *CD4* silencing, but does not necessarily prove its role in the differentiation of $CD4^-8^+$ thymocytes per se. In the present study, we created transgenic mice that overexpress *Runx3* and analyzed the development of thymocytes in these animals. In the *Runx3*-transgenic thymus, the number of $CD4^-8^+$ cells was greatly increased, whereas the numbers of $CD4^+8^+$ and $CD4^+8^-$ cells were reduced. The $CD4^-8^+$ transgenic thymocytes contained mature cells with a $TCR^{high}HSA^{low}$ phenotype. These cells were released from the thymus and contributed to the elevated level of $CD4^-8^+$ cells relative to $CD4^+8^-$ cells in the spleen. Runx3 overexpression also increased the number of mature $CD4^-8^+$ thymocytes in mice with class II-restricted, transgenic *TCR* and in mice with a class I-deficient background, both of which are favorable for $CD4^+8^-$ lineage selection. Thus, Runx3 can drive thymocytes to select the $CD4^-8^+$ lineage. This activity is likely to be due to more than a simple silencing of *CD4* gene expression. *The Journal of Immunology,* **2005, 174: 2627–2636.**

Thymocytes pass through multiple, distinct steps of differentiation and gradually develop into immunocompetent T lymphocytes. At each stage of differentiation, thymocytes face fate decisions, such as whether they will survive or die, which lineage they will select, and how they will mature. These events are mostly regulated by a network of signals that are presented to thymocytes as morphogens, cytokines, MHC, and self-Ag peptides (1, 2). The most critical receptors for these signals are the TCR and its coreceptor molecules, CD4 and CD8. Thus, one of the challenging and fascinating steps of thymocyte differentiation is the positive selection of $CD4^+8^+$ double-positive (DP)[3] cells and the subsequent lineage selection to either $CD4^+$ or $CD8^+$ single-positive (SP) cells (3–5). Various transcription factors appear to function coordinately in the regulation of the *TCR*, *CD4*, and *CD8* genes (6, 7).

Recent advances in our understanding of gene regulation in thymocyte differentiation have involved the roles of the Runx family of transcription factors (6). Expression of Runx1 protein is detected in immature, $CD4^-8^-$ double-negative (DN) and premature DP thymocytes, as well as in mature SP thymocytes (8–11). As expected from this expression pattern, Runx1 appears to exert its function at each step of thymocyte differentiation. For example, both the transition of DN cells to the DP stage and the maturation of postselected SP cells are significantly perturbed if the endogenous Runx1 activity in thymus is reduced by artificially expressing a dominant interfering form of Runx1 (8, 11). Each of these steps is normally accompanied by a tremendous amount of cell proliferation, for which Runx1 function is necessary. Conditional targeting of *Runx1* has also revealed that it has an indispensable role in the initial emergence of T-committed cells from stem cells (12).

In contrast to Runx1, the expression of Runx3 protein is detected mainly in the $CD4^-8^+$ subset of thymocytes and splenocytes (9, 10). In accordance with this protein expression profile, $CD4^-8^+$ thymocytes do not develop in the *Runx3* (−/−) thymus (13, 14). Based on an analysis of *CD4* gene regulation, Taniuchi et al. (13) proposed that Runx3 binds to the Runx elements in the *CD4* silencer and represses *CD4* expression. Use of a Morpholino antisense oligonucleotide in an in vitro thymocyte differentiation system also supported the requirement for *Runx3* in the generation of $CD4^-8^+$ cells (10).

These studies clearly implicate Runx3 in the regulation of *CD4* expression, but do not necessarily prove its role in the differentiation of $CD4^-8^+$ thymocytes per se. Loss-of-function experiments provide information about what Runx3 does but not about everything it can do. In the present study, we overexpressed a transgenic Runx3 specifically in the T lineage and analyzed the development of the transgenic thymocytes. Runx3 can actively drive thymocytes to the $CD4^-8^+$ lineage, which implies that it does more than simply silencing *CD4* gene expression.

Departments of *Molecular Immunology, and [†]Oncology and Molecular Medicine, and [‡]Animal Research Facility, Institute of Development, Aging and Cancer, Tohoku University, Sendai, Japan; [§]Department of Immunology, Tokai University School of Medicine, Isehara, Japan; and [¶]Center for Experimental Medicine, Institute of Medical Science, University of Tokyo, Tokyo, Japan

Received for publication April 15, 2004. Accepted for publication November 12, 2004.

The costs of publication of this article were defrayed in part by the payment of page charges. This article must therefore be hereby marked *advertisement* in accordance with 18 U.S.C. Section 1734 solely to indicate this fact.

[1] This work was supported in part by research grants from the Ministry of Education, Science, Sports, Culture and Technology, Japan. M.S. is a member in the 21st century Center of Education program, "Center for Innovative Therapeutic Development Towards the Conquest of Signal Transduction Diseases," which is headed by K. Sugamura at Tohoku University.

[2] Address correspondence and reprint requests to Dr. Masanobu Satake, Department of Molecular Immunology, Institute of Development, Aging and Cancer, Tohoku University, 4-1 Seiryo-machi, Aoba-ku, Sendai 980-8575, Japan. E-mail address: satake@idac.tohoku.ac.jp

[3] Abbreviations used in this paper: DP, double positive; SP, single positive; DN, double negative; HA, hemagglutinin; β_2m, β_2-microglobulin; ISP, immature single positive; E, embryonic day; HSA, heat-stable Ag.

0022-1767/05/$02.00

Materials and Methods

Plasmids

The hemagglutinin (HA) tag that represents the epitope of flu virus HA was fused to the N terminus of the murine Runx3 coding region by the PCR method as follows. PCR was performed using a murine *Runx3* cDNA (15) as a template. The sequences of the sense and antisense primers were 5′-GCC GGA TCC GAA TTC ACC ATG TAT CCA TAT GAT GTT CCA GAT TAT GCT ATG CGT ATT CCC GTA GAC CC-3′ and 5′-GCC GGA TCC GAA TTC TTA GTA GGG CCG CCA CAC-3′, respectively. The PCR product was digested with *Bam*HI and subcloned into the *Bam*HI site of pLck (p1017), which harbors the proximal promoter region of the murine *Lck* gene and a poly(A) addition sequence derived from the human growth hormone gene (16). The resulting plasmid was designated *pLck-HA/Runx3*. The accuracy of the modified sequences in the plasmid was confirmed by sequencing. Immunohistochemical staining of cDNA-transfected HeLa cells confirmed the nuclear localization of HA-tagged Runx3 protein (data not shown).

Mice

To generate transgenic mouse lines expressing Runx3, the DNA of *pLck-HA/Runx3* was digested with *Spe*I, and the purified fragment containing the Runx3 expression unit was microinjected into fertilized eggs of C57BL/6 mice. Transgenic founders were identified and crossed to C57BL/6 mice. The presence or absence of the transgene was examined by PCR using genomic DNA as a template. The sense and antisense primers were 5′-CGG GAA TTC ATG TAT CCA TAT GAT GTT CCA GAT TAT GCT ATG CGT ATT CCC GTA GAC CC-3′ and 5′-CCG GAA TTC TTA GTA GGG CCG CCA CAC-3′, respectively, and a 1275-bp fragment was amplified from the transgene. Establishment of the human *CD4*-transgenic mice will be described elsewhere (Y. Iwakura, manuscript in preparation). Briefly, fertilized eggs of C3H/HeN mice were microinjected by the human *CD4* cDNA which harbors the murine *CD4* enhancer/promoter and an *SV40*-derived poly(A) addition signal. *β_2-microglobulin* (β_2m)-deficient mice and *CD4*-deficient mice were purchased from The Jackson Laboratory. The I-A^d-restricted, $OVA_{323-339}$-specific TCR-transgenic mice have been previously reported (17).

Flow cytometrical analysis

Cells were liberated from the thymus and spleen and suspended in PBS containing 0.2% (w/v) BSA. The single-cell suspensions were incubated with appropriately diluted mAbs on ice for 30–60 min. The following fluorescein-conjugated mAbs were used: CyChrom-CD4 (Rm4-5), FITC-CD4 (Rm4-5), PE-CD8a (53-6.7), RED613-CD8a (53-6.7; Invitrogen Life Technologies), PE-TCRβ (H57-597), FITC-CD69 (H1.2F3), FITC-Vβ2 (B20.6), FITC-Vβ3 (KJ25), FITC-Vβ4 (KT4), FITC-Vβ5.1 and -5.2, FITC-Vβ6 (RR4-7), FITC-Vβ7 (TR310), FITC-Vβ8.1 and -8.2 (MR5-2), FITC-Vβ8.3 (1B3.3), FITC-Vβ9 (MR10-2), FITC-Vβ10^b (B21.5), FITC-Vβ11 (RR3-15), FITC-Vβ12 (MR11-1), FITC-Vβ13 (MR12-3), FITC-Vβ14 (14-2), FITC-Vβ17^a (KJ23), FITC-HSA (M1-69), and FITC-human CD4 (Leu3a). Except for RED613-CD8a, the mAbs were purchased from BD Pharmingen. The labeled cells were separated with an analytical flow cytometer (EPICS-XL), and the data were analyzed with EXPO32 software (Beckman Coulter).

Immunoblot analysis and EMSA

The CD4$^-$8$^+$HSA^{low} and CD4$^+$8$^-$HSA^{low} fractions were purified from thymocytes or splenocytes, respectively, using autoMACS (Miltenyi Biotec). Its purity was judged to be >90% by flow cytometry. Protein was extracted from cells using a radioimmunoprecipitation assay solution (50 mM Tris-HCl (pH 7.4), 1% (v/v) Triton X-100, 0.5% (w/v) sodium deoxycholate, 0.1% (w/v) SDS, 150 mM NaCl, 1 μg/ml aprotinin, 1 mM $NaVO_4$, and 1 mM NaF). The other procedures necessary for immunoblot analysis including the electrophoresis, transfer to the filter, and immunoreaction were performed as described previously (18). The raising and characterization of the anti-Runx peptide Ab was also described previously (19). The antiserum raised against the C terminus of murine Runx1 can recognize Runx1, Runx2, and Runx3, because they share the common VWRPY sequence at their extreme C-terminal ends. The anti-tubulin α Ab (Ab-1) was purchased from Oncogene. The procedures for preparing nuclear extracts and for the EMSA were described previously (20). The Runx binding sequence from the *Polyomavirus* enhancer was used as a probe to detect Runx DNA binding activity. The anti-HA mAb 3F10 used for the supershift assay was purchased from Roche Diagnostics.

RT-PCR

Total cytoplasmic RNA was isolated from cells using the ISOGEN reagent (Nippon Gene). cDNAs were synthesized from the RNAs by reverse transcription using Superscript II reverse transcriptase (Invitrogen Life Technologies). The cDNAs were PCR-amplified (25 cycles for each gene) with LA-*Taq* polymerase (Takara), using the following sense and antisense primers to detect transcripts: for *CD4*, 5′-CCT GCG AGA GTT CCC AGA AGA AGA TCA CAG-3′ and 5′-TGA TAG CTC TGC TCT GAA AAC CCA GCA CTG-3′; for *CD8α*, 5′-GGT GAG TCG ATT ATC CTG GGG AGT GGA GAA-3′ and 5′-ACA CAA TTT TCT CTG AAG GTC TGG GCT TGC-3′; for *perforin1*, 5′-CAA GCA GAA GCA CAA GTT CGT-3′ and 5′-CGT GAT AAA GTG CGT GCC ATA-3′; for *GATA3*, 5′-AGG CAA GAT GAG AAA GAG TGC CTC-3′ and 5′-CTC GAC TTA CAT CCG AAC CCG GTA-3′; and for *G3PDH*, 5′-ACC ACA GTC CAT GCC ATC AC-3′ and 5′-TCC ACC ACC CTG TTG CTG TA-3′. The PCR products were run through agarose gels and visualized with ethidium bromide staining.

Chromatin immunoprecipitation assay

A chromatin fraction was prepared from thymocytes, fixed and immunoprecipitated by the anti-Runx or anti-HA Ab, respectively. The procedures were as recommended by the manufacturer of the assay kit (Upstate Cell Signaling Solutions). DNA was purified from the precipitate and processed as a template for PCR to amplify the *CD4* silencer-specific sequence. The primers for PCR were 5′-TGT AGG CAC CCG AGG CAA AG-3′ and 5′-GTT CCA GCA CAG GAG CCC CA-3′. The amplified product was run through agarose gels and transferred to nylon membranes. The membranes were hybridized with ^{32}P-labeled, *CD4* silencer-specific oligonucleotide, 5′-ATA CGA AGC TAG GCA ACA GA-3′.

Results

Overexpression of Runx3 in the T lineage cells

Endogenous expression of Runx3 protein is detected mainly in the CD4$^-$8$^+$ subset of T lymphocytes (9, 10). To artificially overexpress Runx3 in the T cell lineage, we placed the *Runx3* coding

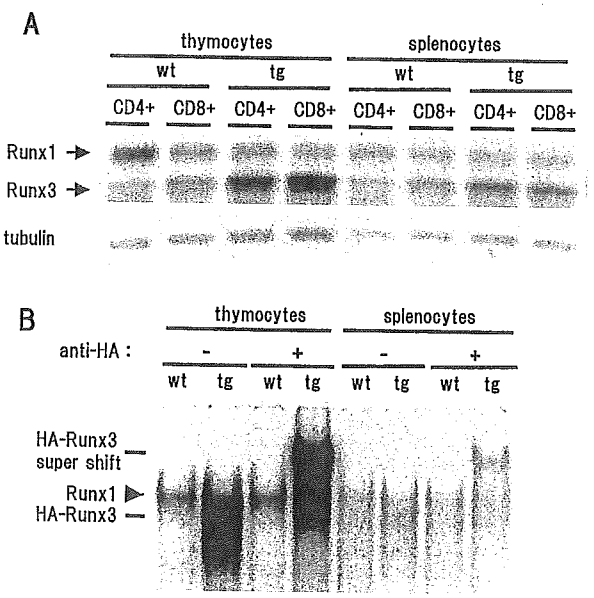

FIGURE 1. Expression of transduced Runx3 protein. *A*, Protein was extracted from thymic and splenic CD4$^+$8$^-$HSA^{low} as well as CD4$^-$8$^+$HSA^{low} cells and processed for immunoblot analysis. The extracts from wild-type and *Runx3*-transgenic cells were probed with an anti-Runx Ab. The bands indicated by the arrows represent the Runx3 and endogenous Runx1 proteins of 52 and 56 kDa, respectively. An immunoblot with an anti-tubulin α Ab served as a control. *B*, Runx DNA binding activity detected by EMSA. The nuclear extracts from the wild-type and *Runx3*-transgenic thymocytes and splenocytes were processed for EMSA. The bands indicated by the arrowhead and bar represent the activity of endogenous Runx1 and transduced HA-Runx3, respectively. The HA-Runx3-derived band was supershifted by the addition of an anti-HA Ab to the transgenic extract.